SUPPLEMENTARY MATERIAL

Neuroimage: Clinical

What graph theory actually tells us about resting state interictal MEG epileptic activity

Guiomar Niso[a,b,*], Sira Carrasco[c], María Gudín[c], Fernando Maestú[a,d], Francisco del-Pozo[a,d], Ernesto Pereda[e]

[a] Center for Biomedical Technology, Technical University of Madrid, Madrid, Spain

[b] McConnell Brain Imaging Center, Montreal Neurological Institute, McGill University, Montreal, Canada

[c] Teaching General Hospital of Ciudad Real, Ciudad Real, Spain

[d] Biomedical Research Networking Center in Bioengineering Biomaterials and Nanomedicine (CIBER-BBN), Madrid, Spain

[e] Electrical Engineering and Bioengineering Group, Dept. of Industrial Engineering, Institute of Biomedical Technology (ITB-CIBICAN), University of La Laguna, Tenerife, Spain

* guiomar.niso@mcgill.ca

1 EPILEPTIC PATIENTS 2

2 DEALING WITH TWO ORTHOGONAL GRADIOMETERS 4

3 STATIONARITY 5

4 PHASE LOCKING VALUE 5

5 THE CHOICE OF AN OPTIMAL DENSITY OF LINKS 6

6 COMPLEX NETWORK INDICES 7

6.1 Degree (D) and Strength (S) 7
6.2 Density (K) 7
6.3 Clustering coefficient (C) 8
6.4 Transitivity (T) 8
6.5 Modularity (Q) 8
6.6 Characteristic path length (L) 9
6.7 Global Efficiency (E_g) 9
6.8 Local Efficiency (E_l) 9
6.9 Eccentricity (ecc), radius and diameter 10
6.10 Betweenness (B) 10
6.11 Eigenvector Spectral centrality (v) 10
6.12 Small worldness (SW) 10
6.13 Algebraic connectivity (ac) 11
6.14 Synchronizability (sync) 12

7 AFFINITY PROPAGATION CLUSTERING 12

8 FALSE DISCOVERY RATE (FDR) 13

9 REFERENCES 14

1 EPILEPTIC PATIENTS

As presented in the paper the study was performed on 45 subjects: 15 patients suffering from frontal focal epilepsy (FE), 15 patients suffering from idiopathic generalized epilepsy (or presumed genetic, as the new terminology stands) (GE) and 15 healthy subjects (HS). A more detailed description of the patients could be seen in Table S1. Abbreviations in this table are as follows:

- AGE: age of the subject
- ED: Education (1: primary, 2: secondary, 3: university)
- GD: Gender (M: male, F: female)
- LAT: Hand laterality (L: left, R: right)
- STA: Age when epilepsy started
- FAM: Family history with epilepsy
- FET: Fetal distress
- PRE: Premaurity
- LESION (RMI): (LF: left frontal, RF: right frontal, DNT: Dysembryoplastic neuroepithelial tumor)
- DIAG: Syndromic diagnosis (FLES: frontal lesional, FNOLES: frontal no lesional)
- STATUS: (C: convulsive, NC: no convulsive)
- CRISIS: (FOC: frontal focal, GEN: generalized)
- FOCAL: (PC: complex partial seizures: "frontal lobe absences", PM: motor partial seizures (hemicorporal clonias), SL: detention of language, OC: oculocephalic version, CA: lift opposite arm (fencing position), AU: somatosensory aura)
- TYPE of GE: (IGE: Idiopathic Generalized Epilepsy, JME: Juvenile Mioclonic Epilepsy, JAE: Juvenile Absence Epilepsy)
- GENERALIZED: (TC: tonic-clonic, MIO: mioclonia, ABS: absence, GM: complex motor generalized during night)
- M: Number of antiepileptic drugs
- AED1: Name of AED1
- AED2: Name of AED2
- Patients marked with * are the ones included in the study

FE	AGE	ED	GD	LAT	STA	FAM	FET	PRE	LESION (MRI)	DIAG	STAT	CRISIS	FOCAL	GENERAL	M	AED1	AED2
EPI_03*	27	3	F	R	12	No	No	No	Parasagittal gliosis LF	FLES	C	FOC, GEN	PC	TC	2	lamotrigina	fenobarbital
EPI_17*	24	3	M	R	16	No	No	No	Venous angioma LP + periatrial gliosis	FLES	No	FOC, GEN	PM	TC	1	levetiracetam	X
EPI_18*	57	3	M	R	18	No	No	No	Normal	FNOLES	NC	FOC, GEN	PC	TC	2	valproico	lamotrigina
EPI_19	46	3	F	R	43	No	No	No	Normal	FNOLES	NC	FOC, GEN	PC	TC	1	valproico	X
EPI_20	59	2	M	R	47	No	No	No	Polymicrogyria LF	FLES	C	FOC, GEN	SL, OC, PC	TC	1	lamotrigina	X
EPI_21*	52	2	F	R	34	No	No	No	Heterotopia RF	FLES	No	FOC, GEN	PC	TC	1	carbamacepina	X
EPI_22*	29	2	M	R	14	No	No	No	Atrophy LF	FLES	No	FOC, GEN	PC	GM	2	valproico	lacosamida
EPI_23	27	2	M	L	15	No	No	No	Displasia cortical RF	FLES	No	FOC, GEN	PM	TC	2	valproico	lamotrigina
EPI_25	38	3	M	R	33	Yes	No	No	Quistica subependimaria RF	FLES	No	FOC, GEN	PM	GM	1	levetiracetam	valproico
EPI_26*	23	2	F	L	17	No	No	No	Angioma RF	FLES	No	FOC	SL, PM	No	2	valproico	lamotrigina
EPI_27*	46	2	F	R	43	No	No	No	Normal	FNOLES	No	FOC, GEN	OC	TC	1	levetiracetam	X
EPI_28*	21	3	M	R	20	No	No	No	Heterotopia LF	FLES	No	FOC, GEN	CA, OC	TC	1	levetiracetam	X
EPI_29*	22	3	M	R	18	No	No	No	Venous angioma LF	FLES	No	GEN	SL	TC	1	valproico	X
EPI_30*	25	3	M	R	14	No	No	No	Normal	FNOLES	No	FOC, GEN	CA, OC	TC	2	valproico	lacosamida
EPI_31*	22	2	M	R	19	Yes	Yes	Yes	Angioma RF	FLES	No	GEN	No	TC	2	valproico	levetiracetam
EPI_32*	69	3	F	R	59	No	No	No	Cavernoma LF	FLES	C	GEN	SL	TC	1	oxcarbamacepina	X
EPI_33*	27	2	F	R	12	No	No	No	Normal	FNOLES	No	GEN	-	TC	2	lamotrigina	valproico
EPI_34	33	2	F	R	15	No	No	No	DNT in RFP to cortical displasia	FLES	No	FOC	AU	No	2	pregabalina	topiramato
EPI_35*	58	2	M	R	18	No	No	No	Vascular malform RF (hemangioma)	FLES	No	FOC	SL	No	2	valproico	fenobarbital

GE	AGE	ED	GD	LAT	STA	FAM	FET	PRE	LESION (MRI)	DIAG	MIO	CRISIS	TYPE	GENERAL	M	AED1	AED2
EPI_01*	28	3	M	R	13	No	No	No	Normal	IGE	Yes	GEN, MIO	JME	TC, MIO	1	levetiracetam	X
EPI_02	20	2	M	R	14	No	No	No	Normal	IGE	Yes	GEN, MIO	JME	TC, MIO	1	valproico	X
EPI_04	27	2	F	R	17	No	No	No	Normal	IGE	Yes	GEN, MIO	JME	TC, MIO	2	valproico	lamotrigina
EPI_05*	20	2	M	R	12	Yes	No	No	Normal	IGE	Yes	GEN, MIO	JME	TC, MIO	1	valproico	X
EPI_06*	24	2	F	R	16	No	No	No	Normal	IGE	No	GEN, MIO	IGE	TC	1	valproico	X
EPI_07*	31	2	F	R	12	No	Yes	No	Normal	IGE	Yes	GEN, MIO	IGE	TC, MIO	2	valproico	levetiracetam
EPI_08	23	2	M	R	-	Yes	No	No	Normal	IGE	Yes	GEN, MIO	IGE	TC, MIO	2	valproico	lamotrigina
EPI_09*	33	3	F	R	11	Yes	No	No	Normal	IGE	Yes	GEN, MIO	JAE	ABS, TC	1	lamotrigina	X
EPI_10*	24	2	F	R	14	Yes	No	No	Normal	IGE	No	ABS	JAE	ABS, TC	1	etosuximida	X
EPI_11*	22	2	F	R	14	Yes	No	No	Normal	IGE	No	GEN	IGE	TC	2	lamotrigina	levetiracetam
EPI_12*	25	2	F	R	13	No	No	No	Normal	IGE	Yes	GEN, MIO	JME	TC, MIO	2	levetiracetam	topiramato
EPI_13*	31	3	M	R	18	No	Yes	No	Normal	IGE	No	GEN	IGE	TC	1	levetiracetam	X
EPI_14*	23	3	F	R	18	Yes	No	No	Normal	IGE	Yes	GEN, MIO	IGE	TC, MIO	1	levetiracetam	X
EPI_15*	20	2	F	R	18	No	No	No	Normal	IGE	No	GEN	JME	TC	1	levetiracetam	X
EPI_16*	29	3	F	R	14	No	No	No	Normal	IGE	Yes	GEN, MIO	JME	TC, MIO	2	levetiracetam	lamotrigina
EPI_36*	46	3	F	R	15	No	No	No	Normal	IGE	Yes	GEN, MIO	IGE	TC, MIO	1	valproico	X
EPI_37	22	2	F	R	10	Yes	No	No	Normal	IGE	No	GEN, ABS	JAE	ABS, TC	2	etosuximida	lacosamida
EPI_38	29	2	M	R	11	Yes	No	No	Normal	IGE	Yes	GEN, MIO	JME	TC, MIO	2	valproico	clobazam
EPI_39	22	3	F	R	10	No	No	No	Normal	IGE	Yes	GEN, MIO	JME	TC, MIO	1	levetiracetam	X
EPI_40	26	2	F	R	14	No	No	No	Normal	IGE	Yes	GEN, MIO	IGE	TC, MIO	2	valproico	levetiracetam
EPI_41*	40	2	M	R	15	No	No	No	Normal	IGE	Yes	GEN, MIO	IGE	TC, MIO	1	levetracetam	X

Table S1: Frontal focal epilepsy (FE) and Generalized epilepsy (GE) subjects

2 DEALING WITH TWO ORTHOGONAL GRADIOMETERS

In this study, we used planar gradiometers instead of magnetometers, due to the reduced sensitivity to deep sources. Yet, as commented in the Method section of the paper, there is no consensus in the literature as to what is the best strategy to combine the information of the two orthogonal gradiometers in connectivity analyses. To compare the effect of different common strategies to deal with this problem on the temporal and spectral profile of the data, Figure S1 shows the time series and the power spectrum of each individual planar gradiometer g_x and gy, their first principal component g_{PC} and its absolute, and their amplitude (or RMS), defined as RMS = $\sqrt{g_x^2 + g_y^2}$.

As expected, the temporal and spectral profile of g_{PC} clearly mirror those of both gradiometers, while at the same time explaining an important percentage of the total variance of both signals (panel D), and reducing the information to a single time series per sensor site. Instead, both its absolute value and the RMS, which are almost identical, modify the temporal course and most importantly the spectrum (panel C), which may be problematic to draw conclusions in the PS analysis. Therefore, we decided to use PCA as an objective method to combine the information from both planar gradiometers with minimum signal distortion in time and frequency domain.

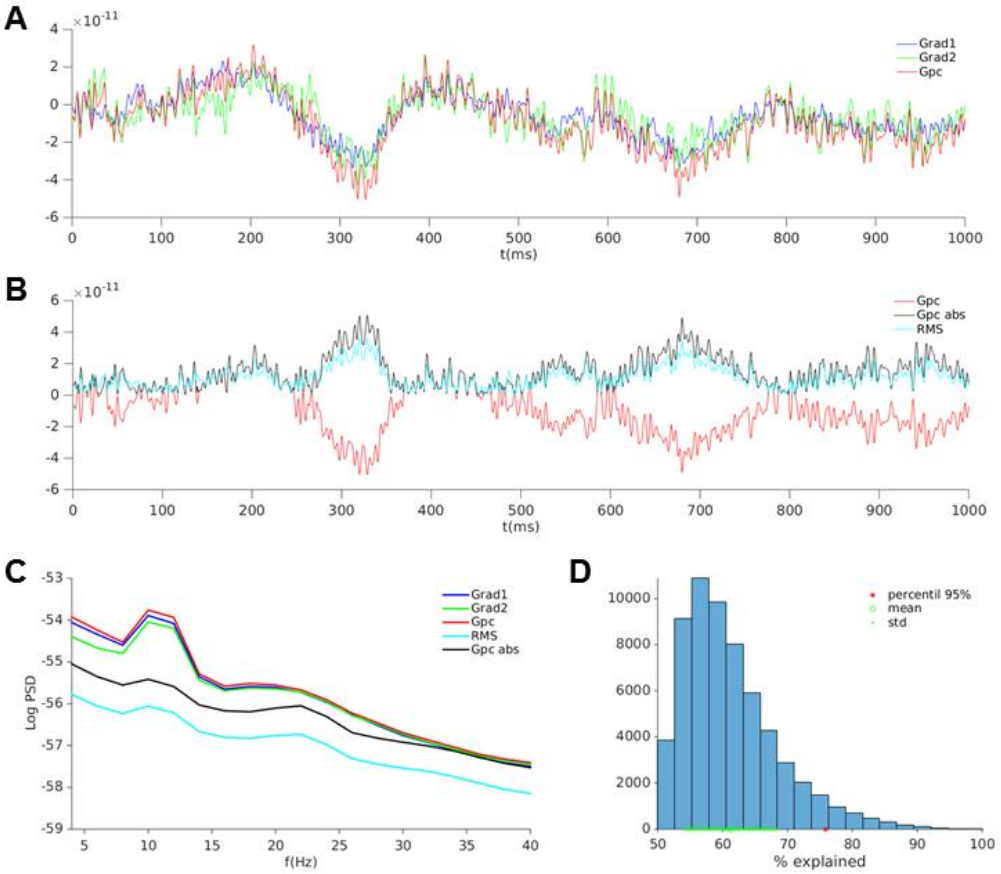

Fig. S1: Dealing with planar gradiometers

A) Signals obtained from two planar gradiometers (Grad1 and Grad2), and their principal component (Gpc), for 1000ms of recording in one channel. B) The same period of time for Gpc, its absolute value (Gpc abs) and the RMS. C) Total PSD for the average of the 102 sensors, 40 trials of 5s each for one subject. D) Histogram for the explained percentage of the total variance by the first principal component of the two gradiometers (Gpc) for the same dataset as in C.

3 STATIONARITY

One important (but often neglected) question, which must be tackled during the preprocessing of the data, is its stationarity. The human brain is a non-stationary system, but for most indices of brain activity from M/EEG at least approximate stationarity is required. In the case of connectivity indexes, stationarity is not always a pre-requisite for their calculation (e.g., those PS indexes where the phase obtained by means of the Hilbert Transform). But certainly, if a given time series is not stationary, the possibility of different brain states being mixed up in it cannot be ruled out. A recent result on spontaneous and evoked MEG activity (Kipiński et al., 2011) has shown that, whereas these data tend to be mean stationary, they are also mostly variance-nonstationary especially for long segments (i.e., longer than 1s). Here, we dealt with this issue by means of the KPSS test (Kwiatkowski et al., 1992), which has been successfully applied to multivariate M/EGG data in recent studies (González et al., 2013; Kipiński et al., 2011). This test calculates a statistic (*ks*), which is later used to decide whether it is possible to reject the null hypothesis of the stationarity of the data at the desired level of statistical significance (see (Kipiński et al., 2011; Kwiatkowski et al., 1992) for technical details). Since the statistics is calculated in univariate time series, we define:

$$\tilde{ks} = \frac{1}{N_s}\sum_{i=0}^{Ns} ks_i \qquad (1)$$

as the statistic for each multivariate (N_S =102 sensors) segment. Then, all the segments were sorted from the lowest to the highest values of the statistic (i.e., from the most to the least stationary segment), and select for further analysis the 40 most stationary segments out of the 100 a priori selected segments. We performed the KPSS analysis with the GCCA toolbox (Seth, 2010).

4 PHASE LOCKING VALUE

In this work we use the Phase Locking Value (PLV) as a measure of phase synchronization (PS) between signals (see, e.g., (Niso et al., 2013) for details). PS refers to a situation when the phases of two coupled oscillators synchronizes, even though their amplitudes may remain uncorrelated (Rosenblum et al., 1996). The PLV makes use only of the relative phase difference between two narrow-band signals (Lachaux, Rodriguez, Martinerie, & Varela, 1999) and it is defined as:

$$PLV = \left|\left\langle e^{i\Delta\phi_{rel}(t)}\right\rangle\right| = \left|\frac{1}{N}\sum_{n=1}^{N} e^{i\Delta\phi_{rel}(t_n)}\right| = \sqrt{\left\langle\cos\Delta\phi_{rel}(t)\right\rangle^2 + \left\langle\sin\Delta\phi_{rel}(t)\right\rangle^2} \qquad (2)$$

where < .> indicates time average. The PLV estimates how the relative phase is distributed over the unit circle and it has been computed using HERMES toolbox (Niso et al., 2013), available at http://hermes.ctb.upm.es/.

5 THE CHOICE OF AN OPTIMAL DENSITY OF LINKS

As commented in the manuscript (cfr. Section 2.8, *Functional brain networks*), the problem of finding an appropriate significance threshold for the links of a reconstructed functional brain network remains open. Most studies in the literature, however, take into account the results presented in (van Wijk et al., 2010), and use a fixed density approach, whereby the same number of links are used across groups and conditions. Recently, (Kim et al., 2013), analyzing epileptic brain networks from EEG data, have demonstrated that many brain network measures reach a maximum for a density slightly above the minimum value k_{ER} =2lnN/N defined in the Erdös-Renyi model (Erdös and Renyi, 1961) for a random graph of N nodes to become fully connected (in our case, k_{ER} ~ 0.1). Besides, (Zhang et al., 2011) have also used a relatively low density (i.e., less than 50% of the links) to investigate GE networks using fMRI and DTI, arguing that for such values *"all functional (...) connectivity networks were fully connected and with a minimum number of spurious edges"*. Thus, in this work we selected *k=0.35*, following these references. As shown in Figure S2, the results of the network measures singled out by the affinity propagation method (AP, see below) are robust for values of *k* around the selected one.

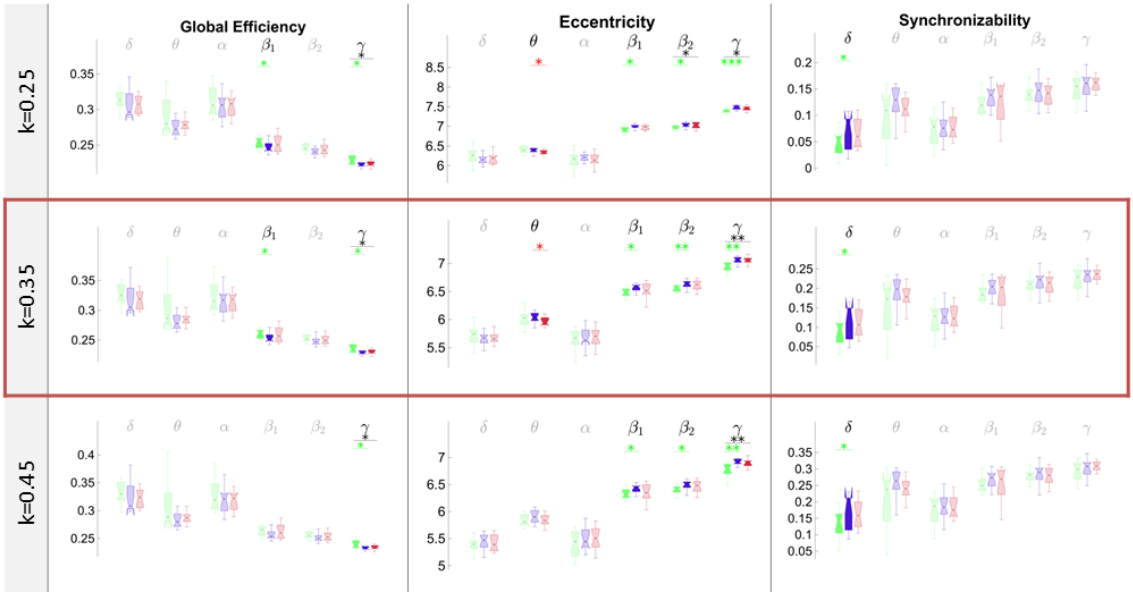

Fig. S2: Results for different density of links for the FC matrix

Results for the three representants of the complex networks groups (Global Efficiency, Eccentricity and Synchronizability), for density values k=0.25, k=0.35 (value actually used) and k=0.45.

6 COMPLEX NETWORK INDICES

To characterize neural networks in this work we calculated many of the indices most commonly used for this purpose: the average degree *(D)*, the strength *(S)*, the clustering coefficient *(C)*, the transitivity *(T)*, the local efficiency *(E)* , the modularity *(Q)*, the characteristic path length *(L)*, the global efficiency *(E_g)*, the eccentricity *(ecc)*, the network radius *(rad)* and diameter *(diam)*, the betweenness *(B)* and the eigenvalue spectral density *(v)*. Here we describe the details for each of them.

Before starting, some notation is explained for a given graph G with the adjacency matrix A (see (Rubinov and Sporns, 2010) for details):

- *N* is the set of all nodes in the network, and *n* is the number of nodes.
- *L* is the set of all links in the network, and *l* is number of links.
- *(i, j)* is a link between nodes *i* and *j*, *($i, j \in N$)*.
- Links *(i, j)* are associated with connection weights w_{ij}.
- a_{ij} is the connection status between *i* and *j*: $a_{ij}=1$ when link *(i, j)* exists (when *i* and *j* are neighbors); $a_{ij}=0$ otherwise *($a_{ii}=0$ for all i)*.

We compute the number of links as $l=\boldsymbol{\Sigma}_{i,j\in N} a_{ij}$ (to avoid ambiguity with directed links we count each undirected link twice, as a_{ij} and as a_{ji}). The sum of all weights in the network is l^w, and it is computed as $l^w=\boldsymbol{\Sigma}_{i,j\in N} w_{ij}$. Henceforth, I assume that weights are normalized, such that $0\leq w_{ij}\leq 1$ for all *i* and *j*.

All the following definitions are specifically for weighted undirected graphs.

6.1 Degree (D) and Strength (S)

The *degree* (D) of a node is the number of links connected to it.

$$d_i = \sum_{j\in N} a_{ij} \qquad D = \frac{1}{N}\sum_{i=1}^{N} d_i \tag{3}$$

The global degree of a network is the average of all its nodes' degree. Note that connection weights are ignored in calculations. The mean network degree is most commonly used as a measure of *density* (see 6.2), or the total "wiring cost" of the network. The weighted variant of the degree, sometimes termed the *strength* (S), is defined as the sum of weights of links connected to the node.

$$S_i = d_i^w = \sum_{j\in N} w_{ij} \tag{4}$$

6.2 Density (K)

Density (K) is the fraction of present connections to possible connections. It ranges between 0 and 1, being 0 a totally disconnected network and 1 a totally regular network in which every node is connected to all the others.

$$k_i = \frac{d_i}{N-1} \qquad K = \frac{1}{N}\sum_{i=1}^{N} k_i = \frac{D}{N(N-1)} \tag{5}$$

6.3 Clustering coefficient (C)

The *clustering coefficient* (C) describes the likelihood that neighbours of a vertex are also connected. It is the fraction of triangles around a node, and is equivalent to the fraction of node's neighbours that are neighbours of each other. It quantifies the tendency of network elements to form local clusters.

We used here the weighted version of this measure (Onnela et al., 2005), which characterizes local clustering as:

$$C^{w} = \frac{1}{n}\sum_{i \in N} C_i^{w} = \frac{1}{n}\sum_{i \in N} \frac{2t_i^{w}}{k_i(k_i - 1)} \tag{6}$$

where C_i is the clustering coefficient of node i (C_i =0 for $k_i < 2$), and the number of triangles t_i^w around a node i, is defined by the geometric mean of triangles around it:

$$t_i^{w} = \frac{1}{2}\sum_{j,h \in N} \left(w_{ij} w_{ih} w_{jh}\right)^{1/3} \tag{7}$$

Triangles are important since they are directly related to the robustness and error tolerance of the network (Boccaletti et al., 2006).

The superscript '*w*' denotes that the indexes are calculated for weighted networks.

6.4 Transitivity (T)

The *transitivity* (T) is the ratio of triangles to triplets in the network and it is an alternative to the clustering coefficient (e.g., (Newman, 2003)). Note that transitivity is not defined for individual nodes, it is only a global measure.

$$T^{w} = \frac{\sum_{i \in N} 2t_i^{w}}{\sum_{i \in N} k_i(k_i - 1)} \tag{8}$$

6.5 Modularity (Q)

The optimal community structure is a subdivision of the network into non-overlapping groups of nodes in a way that maximizes the number of within-group edges, and minimizes the number of between-group edges. The *modularity* (Q) is a statistic that quantifies the degree to which the network may be subdivided into such clearly delineated subgroups or modules. We used a modification for weighted networks by (Newman, 2004):

$$Q^{w} = \frac{1}{l^{w}}\sum_{i,j \in N} \left[w_{ij} - \frac{k_i^{w} k_j^{w}}{l^{w}} \right] \delta_{m_i m_j} \tag{9}$$

Roughly speaking, the greater the value of Q, the more modular a network is, i.e., the greater the density of within-group connections as compared to the between-group ones.

6.6 Characteristic path length (L)

To define this index, it is necessary to first introduce the notion of 'path'. A *path* consists of a sequence of linked nodes that never visit a single node more than once. It is important, to differentiate it from 'walks', which are sequences of linked nodes that may visit a single node more than once. The *characteristic path length*, then, is defined as the average shortest path length in the network (Watts and Strogatz, 1998).

$$L^{w} = \frac{1}{N}\sum_{i \in N} L_i^{w} = \frac{1}{n}\sum_{i \in N} \frac{\sum_{\substack{j \in N \\ i \neq j}} d_{ij}^{w}}{n-1} \tag{10}$$

where L_i is the average distance between node i and all other nodes. The shortest weighted path length between i and j, is defined as:

$$d_{ij} = \sum_{a_{uv} \in g_{i \leftrightarrow j}} f(w_{uv}) \tag{11}$$

where f is a map (e.g., an inverse) from weight to length and $g_{i \leftrightarrow j}$ is the shortest weighted path between i and j. . Here we followed the suggestion of (Boccaletti et al., 2006), and set the length of the edge connecting nodes i and j inversely proportional to the weight: $d_{ij} = 1/w_{ij}$. The shortest path length quantifies the extent of average connectivity or the overall routing efficiency of the network (Achard and Bullmore, 2007).

6.7 Global Efficiency (E_g)

The *global efficiency* (E_g) is related to the previous index, as it is defined as the average inverse shortest path length in the network, hence they will be inversely correlated (Latora and Marchiori, 2001).

$$E_g^{w} = \frac{1}{N}\sum_{i \in N} E_i^{w} = \frac{1}{N}\sum_{i \in N} \frac{\sum_{\substack{j \in N \\ i \neq j}} \left(d_{ij}^{w}\right)^{-1}}{N-1} \tag{12}$$

where E_i is the efficiency of node i. It reflects the global efficiency of parallel information transfer in the network.

6.8 Local Efficiency (E_l)

The *local efficiency (E)* is the global efficiency (see 6.7) computed on node neighbourhoods, so it will be related to the clustering coefficient (6.3) (Latora and Marchiori, 2001).

$$E_l^{w} = \frac{1}{N}\sum_{i \in N} E_{loc,i}^{w} = \frac{1}{N}\sum_{i \in N} \frac{\sum_{\substack{j,h \in N \\ i \neq j}} \left(w_{ij} w_{ih} - \left[d_{jh}^{w}(N_i)\right]^{-1}\right)^{1/3}}{k_i^{w}(k_i^{w}-1)} \tag{13}$$

where $E_{loc,i}$ is the local efficiency of node *i*, and $d_{jh}(N_i)$ is the length of the shortest path between *j* and *h*, that contains only neighbours. The local efficiency can be understood as a measure of the fault tolerance of the network, indicating how well each subgraph exchanges information when the index node is eliminated (Achard and Bullmore, 2007).

6.9 Eccentricity (ecc), radius and diameter

The node eccentricity is the maximal shortest path length (see 6.6) between a node and any other node. The lower the eccentricity, the more central a vertex is in a network. The *radius* is the minimum eccentricity and the *diameter* is the maximum eccentricity (see above).

6.10 Betweenness (B)

Node *betweenness centrality* (B) is the number of all shortest paths in the network that contain a given node. Nodes with high values of betweenness centrality participate in a large number of shortest paths. It can be defined as in (e.g., (Freeman, 1979))

$$b_i = \frac{1}{(N-1)(N-2)} \sum_{\substack{h,j \in N \\ h \neq j, h \neq i, j \neq i}} \frac{\rho_{hj}(i)}{\rho_{hj}} \qquad (14)$$

where ρ_{hj} is the number of shortest paths between nodes *h* and *j*, and $\rho_{hj}(i)$ is the number of shortest paths between these two nodes that pass through node *i*. As an example of application to MEG data in epilepsy, this index has been recently used, along with the minimum spanning tree, to assess the outcome of surgery in a follow up study of lesional epilepsy patients (van Dellen et al., 2014).

6.11 Eigenvector Spectral centrality (v)

Eigenvector centrality (v) is a self-referential measure of centrality. It determines the importance of a node on the basis of its connections to other nodes, but also with respect to how those other nodes are connected (and so on). It weighs the connections of a node (Bonacich, 2007), so that when connected to a highly connected "hub" makes it more influential than being connected to many poorly connected peripheral nodes. In this way, eigenvector centrality takes the relation within the whole network into account and allows for the identification of hubs (Hardmeier et al., 2012).

6.12 Small worldness (SW)

Network *small-worldness* (Humphries and Gurney, 2008; Watts and Strogatz, 1998)

$$SW = \frac{C / C_{rand}}{L / L_{rand}} \qquad (15)$$

where C and C_{rand} are the clustering coefficients, and L and L_{rand} are the characteristic path lengths of the respective tested network and a random network. Small-world networks often have S≫1.

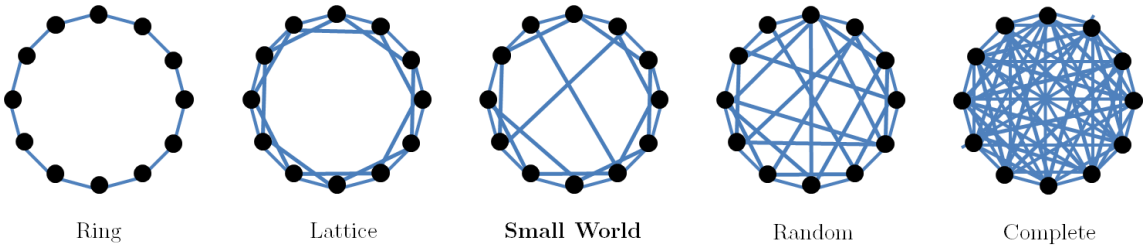

Fig. S3: Small world networks

Small-world property is characterized by a high local clustering of connections between neighboring nodes and short path lengths between any pair of nodes. It was after (Watts and Strogatz, 1998) introduced this concept, that it has been observed in many complex networks of nature, including social, economic and biological networks. The cortical networks of other mammalian brains as well as functional and structural human brain networks have been found to exhibit small-world properties (Li et al., 2009).

A real network would be considered as small-world if it meets the $C_r=\gamma=C/C_{rand}>>1$ and $L_r=\lambda=L/L_{rand}=1$, in which C_{rand} and L_{rand} are the mean clustering coefficient and mean shortest path length of the random network (Watts and Strogatz, 1998). For the calculation of C_{rand} and L_{rand}, we generated 50 random networks for each subject's functional connectivity matrix by a randomization (using BCT toolbox (Rubinov and Sporns, 2010)), in which the original connectivity matrix was randomly permuted (randomly reshuffling links), while keeping the degree distribution of each node constant (Fornito et al., 2013; Maslov and Sneppen, 2002; Rubinov and Sporns, 2010). Then, the average across all 50 generated random networks was performed to obtain the mean C_{rand} and L_{rand} indexes, and thus the small-world indices C_r and L_r were calculated for the weighted FC networks.

6.13 Algebraic connectivity (ac)

Now we will introduce two parameters (algebraic connectivity, this section, and synchronizability, next section) based on the *spectral graph theory*, which studies the properties of graphs via the eigenvalues and eigenvectors of their associated graph matrices: the adjacency matrix (A) and the combinatorial Laplacian matrix (L), also known as Kirchhoff matrix (since it was originally proposed by Kirchhoff) and its variants. The connection between the Laplacian and the adjacency matrices is L = D – A, where D is the diagonal degree matrix D := D_{ii}, being D_{ii} the strength of node *i*.

We denote the set of eigenvalues of the adjacency matrix A as $\lambda_1 \leq \lambda_2 \leq \cdots \leq \lambda_N$, where the largest eigenvalue λ_N is called *the spectral radius*; and the eigenvalues of the Laplacian matrix L as $0=\mu_1 \leq \mu_2 \leq \cdots \leq \mu_N$. The eigenvalues of the adjacency matrix are real, while the eigenvalues of the Laplacian matrix are real and non-negative. (see (Boccaletti et al., 2006) for details).

The largest eigenvalue μ_N characterizes dynamic processes on networks such as virus spreading and synchronization processes. Its inverse, $1/\mu_N$, describes the threshold of the phase transition,

which specifies the onset of a remaining fraction of infected nodes and of locked oscillators, respectively, of both virus spread and synchronization of coupled oscillators in networks (Li et al., 2011).

The *algebraic connectivity* (*ac*), measures how difficult it is to tear a network apart (Fiedler, 1973). The algebraic connectivity is defined as the second smallest eigenvalue of the Laplacian matrix, μ_2. It is greater than 0 if and only if the network is fully connected.

$$ac = \mu_2 \tag{16}$$

The magnitude of the algebraic connectivity is important for synchronization, and reflects also network robustness (resilience against damage).

6.14 Synchronizability (sync)

The term '*synchronizability*' is often used for the ratio of Laplacian's largest and second smallest eigenvalues μ_N and μ_2, respectively. It gives the idea of the stability of a graph. The larger the ratio, the more difficult to synchronize the oscillators; the smaller it is, the more stable the network synchronization (Arenas et al., 2008).

$$R = \frac{\mu_N}{\mu_2} \tag{17}$$

This ratio is also referred to as the '*paradox of heterogeneity*'. It shows that (unweighted, undirected) networks with a more homogeneous degree distribution synchronize more easily than networks with a more heterogeneous degree distribution (Li et al., 2011; Mieghem, 2012). This index has been recently used in neuroscience (de Haan et al., 2012; Lehnertz et al., 2014; Li et al., 2011). Here, however, we will used the inverse (17) following (De Haan, 2012), to obtain an index ranging between 0 and 1, which is closer to 1 when the network is easier to synchronize.

$$sync = \frac{1}{R} \tag{18}$$

7 AFFINITY PROPAGATION CLUSTERING

The Affinity propagation (AP) is a recently described clustering data method that takes as input measures the similarity between pairs of data points and simultaneously considers all data points as potential exemplars, in contrast to traditional data clustering algorithms. Real-valued messages are exchanged between data points until a high-quality set of exemplars and corresponding clusters gradually emerges. It has been used to solve a variety of clustering problems[1] and it was been shown to uniformly find clusters with much lower error than other methods, in less than one-hundredth the

[1] see http://www.psi.toronto.edu/index.php?q=affinity%20propagation

amount of time (Frey and Dueck, 2007; Givoni and Frey, 2009). In our particular application, AP presents three additional advantages: first, it works with similarities (i.e., correlations between the data, instead of distances); second, it is adaptive to the data; and third, it is not necessary to fix a priori the number of clusters, but the algorithm determines, in a purely data-driven way, the optimal number of clusters, thereby providing a direct answer to our question of how many different networks measures are enough to fully describe the data. This allows us to reduce the number of graph theoretical network measures to be further analysed in the epileptic study, by selecting only one representative from each cluster.

8 FALSE DISCOVERY RATE (FDR)

To correct for multiple comparisons, as a consequence of multiple hypothesis testing, we used the false discovery rate (FDR) method (Benjamini and Yekutieli, 2001; Genovese et al., 2002). FDR controls the expected proportion of incorrectly rejected null hypotheses (type I errors) among all rejected hypotheses. In this case we have used the type I FDR implementation (Genovese et al., 2002), since the results of the p values are very likely to be positively correlated, as the noise in the data is Gaussian with non-negative correlation across sensors (Benjamini and Yekutieli, 2001), and two close close sensors (and the PLV between close sensors) are likely to reflect partially overlapping information. Table S2 summarizes the information regarding the statistics applied to the data in the study.

GLOBAL	Power spectrum		**Wilcoxon** HS vs GE HS vs FE GE vs FE	⇨ **FDR type I (q<0.05)** 4:2:40 Hz
	Networks indices		**Wilcoxon** HS vs GE HS vs FE GE vs FE	⇨ **FDR type I (q<0.1)** 4:4:40 Hz
LOCAL	Power spectrum		**Wilcoxon** HS vs GE HS vs FE GE vs FE	⇨ **FDR type I (q<0.05)** 1:102 channels
	Networks indices	NODES	**Wilcoxon** HS vs GE HS vs FE GE vs FE	⇨ **FDR type I (q<0.1)** 1:102 channels
		EDGES	**Non parametric permutation test**	

Table S2: Summary of the statistical tests applied to the data

9 REFERENCES

Achard, S., Bullmore, E., 2007. Efficiency and cost of economical brain functional networks. PLoS Comput. Biol. 3, e17. doi:10.1371/journal.pcbi.0030017

Arenas, A., Díaz-Guilera, A., Kurths, J., Moreno, Y., Zhou, C., 2008. Synchronization in complex networks. Phys. Rep. 469, 93–153. doi:10.1016/j.physrep.2008.09.002

Benjamini, Y., Yekutieli, D., 2001. The control of the false discovery rate in multiple testing under dependency. Ann. Stat. 29, 1165–1188.

Boccaletti, S., Latora, V., Moreno, Y., Chavez, M., Hwang, D., 2006. Complex networks: Structure and dynamics. Phys. Rep. 424, 175–308. doi:10.1016/j.physrep.2005.10.009

Bonacich, P., 2007. Some unique properties of eigenvector centrality. Soc. Networks 29, 555–64. doi:10.1016/j.socnet.2007.04.002

De Haan, W., 2012. In a Network State of Mind. Vrije Universiteit Amsterdam.

De Haan, W., van der Flier, W.M., Koene, T., Smits, L.L., Scheltens, P., Stam, C.J., 2012. Disrupted modular brain dynamics reflect cognitive dysfunction in Alzheimer's disease. Neuroimage 59, 3085–3093.

Erdős, P., Renyi, A., 1961. On the strength of connectedness of a random graph. Acta Math. Hungarica 12, 261–267.

Fiedler, M., 1973. Algebraic connectivity of graphs. Czechoslov. Math. J. 23.

Fornito, A., Zalesky, A., Breakspear, M., 2013. Graph analysis of the human connectome: promise, progress, and pitfalls. Neuroimage 80, 426–44. doi:10.1016/j.neuroimage.2013.04.087

Freeman, L.C., 1979. Centrality in social networks conceptual clarification. Soc. Networks 1, 215–239.

Frey, B.J., Dueck, D., 2007. Clustering by passing messages between data points. Science (80-.). 315, 972–6. doi:10.1126/science.1136800

Genovese, C.R., Lazar, N. a, Nichols, T., 2002. Thresholding of statistical maps in functional neuroimaging using the false discovery rate. Neuroimage 15, 870–8. doi:10.1006/nimg.2001.1037

Givoni, I., Frey, B., 2009. A binary variable model for affinity propagation. Neural Comput. 1600, 1589–1600.

González, J.J., Méndez, L.D., Mañas, S., Duque, M.R., Pereda, E., De Vera, L., 2013. Performance analysis of univariate and multivariate EEG measurements in the diagnosis of ADHD. Clin. Neurophysiol. 124, 1139–50. doi:10.1016/j.clinph.2012.12.006

Hardmeier, M., Schoonheim, M.M., Geurts, J.J.G., Hillebrand, A., Polman, C.H., Barkhof, F., Stam, C.J., 2012. Cognitive dysfunction in early multiple sclerosis: altered centrality derived from resting-state functional connectivity using magneto-encephalography. PLoS One 7, e42087. doi:10.1371/journal.pone.0042087

Humphries, M.D., Gurney, K., 2008. Network "small-world-ness": a quantitative method for determining canonical network equivalence. PLoS One 3, e0002051. doi:10.1371/journal.pone.0002051

Kim, D.-J., Bolbecker, A.R., Howell, J., Rass, O., Sporns, O., Hetrick, W.P., Breier, A., O'Donnell, B.F., 2013. Disturbed resting state {EEG} synchronization in bipolar disorder: A graph-theoretic analysis. NeuroImage Clin. 2, 414–423. doi:http://dx.doi.org/10.1016/j.nicl.2013.03.007

Kipiński, L., König, R., Sielużycki, C., Kordecki, W., 2011. Application of modern tests for stationarity to single-trial MEG data: transferring powerful statistical tools from econometrics to neuroscience. Biol. Cybern. 105, 183–95. doi:10.1007/s00422-011-0456-4

Kwiatkowski, D., Phillips, P.P.C.B., Schmidt, P., Shin, Y., 1992. Testing the null hypothesis of stationarity against the alternative of a unit root: How sure are we that economic time series have a unit root? J. Econom. 54, 159–178.

Latora, V., Marchiori, M., 2001. Efficient behavior of small-world networks. Phys. Rev. Lett. 87, 198701. doi:10.1103/PhysRevLett.87.19870

Lehnertz, K., Ansmann, G., Bialonski, S., 2014. Evolving networks in the human epileptic brain. Phys. D Nonlinear Phenom. 267, 7–15.

Li, C., Wang, H., de Haan, W., Stam, C.J., Mieghem, P. van, 2011. The correlation of metrics in complex networks with applications in functional brain networks. J. Stat. Mech. 2011, P11018.

Li, Y., Liu, Y., Li, J., Qin, W., Li, K., Yu, C., Jiang, T., 2009. Brain anatomical network and intelligence. PLoS Comput. Biol. 5, e1000395. doi:10.1371/journal.pcbi.1000395

Maslov, S., Sneppen, K., 2002. Specificity and stability in topology of protein networks. Science (80-.). 296, 910–3.

Mieghem, P. van, 2012. Graph Spectra for Complex Networks. Cambridge University Press.

Newman, M., 2003. The structure and function of complex networks. SIAM Rev. 45, 167–256.

Newman, M., 2004. Fast algorithm for detecting community structure in networks. Phys. Rev. E 69, 066133. doi:10.1103/PhysRevE.69.066133

Niso, G., Bruña, R., Pereda, E., Gutiérrez, R., Bajo, R., Maestú, F., Del-Pozo, F., 2013. HERMES: towards an integrated toolbox to characterize functional and effective brain connectivity. Neuroinformatics 11, 405–434. doi:10.1007/s12021-013-9186-1

Onnela, J., Saramäki, J., Kertész, J., Kaski, K., 2005. Intensity and coherence of motifs in weighted complex networks. Phys. Rev. E 71, 065103(R). doi:10.1103/PhysRevE.71.065103

Rosenblum, M., Pikovsky, A., Kurths, J., 1996. Phase synchronization of chaotic oscillators. Phys. Rev. Lett. 76, 1804–7.

Rubinov, M., Sporns, O., 2010. Complex network measures of brain connectivity: uses and interpretations. Neuroimage 52, 1059–1069. doi:10.1016/j.neuroimage.2009.10.003

Seth, A.K., 2010. A MATLAB toolbox for Granger causal connectivity analysis. J. Neurosci. Methods 186, 262–73. doi:10.1016/j.jneumeth.2009.11.020

Van Dellen, E., Douw, L., Hillebrand, A., de Witt Hamer, P.C., Baayen, J.C., Heimans, J.J., Reijneveld, J.C., Stam, C.J., 2014. Epilepsy surgery outcome and functional network alterations in longitudinal MEG: a minimum spanning tree analysis. Neuroimage 86, 354–363.

Van Wijk, B.C.M., Stam, C.J., Daffertshofer, A., 2010. Comparing Brain Networks of Different Size and Connectivity Density Using Graph Theory. PLoS One 5, e13701. doi:10.1371/journal.pone.0013701

Watts, D.J., Strogatz, S.H., 1998. Collective dynamics of "small-world"networks. Nature 393, 440–442.

Zhang, Z., Liao, W., Chen, H., Mantini, D., Ding, J.R., Xu, Q., Wang, Z., Yuan, C., Chen, G., Jiao, Q., Lu, G., 2011. Altered functional-structural coupling of large-scale brain networks in idiopathic generalized epilepsy. Brain 134, 2912–2928. doi:10.1093/brain/awr223